

Nuclear Magnetic Resonance on Oriented $^{101}\text{Rh}^m$ †

G. Kaindl,* F. Bacon,‡ H.-E. Mahnke,§ and D. A. Shirley

Department of Chemistry and Lawrence Berkeley Laboratory, University of California, Berkeley, California 94720

(Received 16 May 1973)

The 4.3-day isomer of ^{101}Rh was oriented in nickel metal by the thermal equilibrium nuclear orientation technique at temperatures down to 3 mK. From an analysis of the temperature dependence of the anisotropies of the 306.8- and 544.8-keV γ rays of ^{101}Ru , the $E2/M1$ mixing ratios of these two γ transitions, $\delta(306.8) = -0.10 \pm 0.05$ and $\delta(544.8) = -0.98 \pm 0.10$, as well as the magnetic hyperfine interaction of $\text{Ni}(^{101}\text{Rh}^m)$, $|\mu\text{H}| = (6.2 \pm 0.2) \times 10^{-18}$ erg, could be derived. In addition, the previously assigned spins of the respective nuclear states of ^{101}Ru at 306.8 and 544.8 keV were both confirmed as $7/2$. Nuclear magnetic resonance on oriented $\text{Ni}(^{101}\text{Rh})$ was observed in an external polarizing field of 1 kOe at a resonance frequency of 206.2 ± 0.4 MHz, yielding a magnetic hyperfine splitting of $|\mu\text{H}/I| = (1.366 \pm 0.003) \times 10^{-18}$ erg. As a result both the spin and the magnetic moment of $^{101}\text{Rh}^m$ could be determined as $I = 9/2$ and $\mu(9/2) = (+)(5.51 \pm 0.09)\mu_B$, corresponding to a nuclear g factor of $g(9/2) = 1.22 \pm 0.02$. The results confirm the interpretation of $^{101}\text{Rh}^m$ as a $1g_{9/2}$ proton state. The derived value of the g factor is compared with g factors of other $g_{9/2}$ proton states in the neighborhood of the magic proton number 40, and it is found to fit well into the over-all systematics.

I. INTRODUCTION

Thermal-equilibrium nuclear orientation via magnetic hyperfine interaction at dilute impurities in ferromagnetic host metals (NO),¹ especially when combined with the method of nuclear magnetic resonance (NMR-ON)² can be used as a very powerful tool for studying magnetic hyperfine interactions of nuclear isomers with half-lives of a few hours or longer. Both the size of the magnetic hyperfine interaction and the spin of the oriented nucleus can be obtained in this way.³⁻⁵ The degree of nuclear orientation is determined from the anisotropy of nuclear radiations, especially nuclear γ rays, emitted after the decay of the oriented nuclei. Additional information on γ -ray multiplicities and level spins can be obtained from the signs and magnitudes of the observed γ -ray anisotropies.

We have applied this technique to the 157-keV, $T_{1/2} = 4.34$ day isomer of ^{101}Rh ,^{6,7} which decays predominantly by allowed EC decay to excited states of ^{101}Ru . The $^{101}\text{Rh}^m$ nuclei were oriented in nickel metal at temperatures down to 3 mK. Both the temperature dependence of the anisotropy of nuclear γ rays emitted after the decay of oriented $^{101}\text{Rh}^m$ and nuclear magnetic resonance were observed. As a result both the spin and the magnetic moment of the isomeric state could be derived, supporting an interpretation of this state as a $1g_{9/2}$ proton state.⁶ In addition, information was obtained on level spins and γ ray multiplicities in the ^{101}Ru decay scheme.

II. EXPERIMENTAL PROCEDURE

A. Sample Preparation

The 4.34-day $^{101}\text{Rh}^m$ activity was produced by the $^{101}\text{Ru}(d, 2n)^{101}\text{Rh}^m$ reaction at a deuteron energy of 25 MeV. Natural ruthenium metal of 99.999% nominal purity was used as a target material for the cyclotron irradiation, allowing chemical separation of carrier-free $^{101}\text{Rh}^m$ activity. This was achieved with the standard ruthenium-rhodium separation method⁸ with only minor modifications.

The carrier-free $^{101}\text{Rh}^m$ activity was subsequently electroplated onto a nickel foil of nominal 99.999% purity. For the NO experiment this foil was melted in a hydrogen atmosphere together with a matched amount of ^{60}Co in nickel to be used for thermometry. To insure homogeneity, the sample was remelted several times before it was rolled to a foil of about 0.1-mm thickness. Finally, the foil was carefully annealed in a hydrogen atmosphere at about 1200°C. For the NMR-ON experiment no ^{60}Co activity was added to the $\text{Ni}(^{101}\text{Rh}^m)$ sample, and foils of only about 10 000 Å thickness were prepared.

B. NO and NMR-ON Techniques

An adiabatic demagnetization apparatus, using cerium magnesium nitrate (CMN) as a cooling salt, was employed to cool the samples to temperatures as low as 3 mK. Good thermal contact could be established between the paramagnetic salt and the sample by a system of 0.1-mm-thick copper sheets, which were hard-soldered together outside of the

salt pill and machined to a solid rod. The sample was soft-soldered to this copper cold finger with Bi-Cd alloy. An external polarization field could be applied to the sample with the help of a superconducting Helmholtz pair. More details of the low-temperature technique have been described elsewhere.⁴

To measure the temperature dependence of γ -ray anisotropies, spectra were taken for periods of 15 min with the help of high-resolution coaxial Ge(Li) diodes parallel and perpendicular to the polarizing field as the sample warmed up to about 1 K over a typical time span of 8 h. After corrections were made for background and radioactive decay, the anisotropies of the various γ lines were obtained. The relevant lattice temperatures of the sample were determined from the anisotropies of the 1173-keV and 1333-keV γ rays of ^{60}Ni , originating from the decay of oriented ^{60}Co .

For the NMR-ON experiments an rf field was applied perpendicular to the polarizing field, and the amplitude of the rf field was measured with a pickup coil. In these runs a 7.6- \times 7.6-cm NaI(Tl) detector at $\theta=0^\circ$ was employed to improve counting statistics. The NMR-ON resonance was observed by recording the intensity of the 306.8-keV γ rays at $\theta=0^\circ$ as a function of the frequency of the applied rf field. The rf field had an amplitude of approximately 0.4 mOe and was modulated in saw-tooth form over a bandwidth of 1 or 2 MHz with a modulation frequency of 100 Hz.

C. Decay Scheme of $^{101}\text{Rh}^m$

The decay scheme of $^{101}\text{Rh}^m$, taken from Ref. 9, is shown in Fig. 1. The isomeric state of ^{101}Rh decays predominantly via allowed EC decay to ^{101}Ru . The fraction of decays by an isomeric transition to the ground state of ^{101}Rh has been determined as 0.072.¹⁰

In 99% of the EC decays of $^{101}\text{Rh}^m$ the 306.7- and 544.8-keV levels of ^{101}Ru are directly populated. Both levels decay predominantly to the ground state of ^{101}Ru , giving rise to two intense γ lines, which are well suited for anisotropy measurements.

A spin and parity assignment of $\frac{9}{2}^+$ has been made for the 157.3-keV isomeric state of ^{101}Rh ,⁶ and of $\frac{7}{2}^+$ for the 306.8-keV state of ^{101}Ru .¹¹ There has been some ambiguity, however, in the spin assignment for the 544.8-keV state of ^{101}Ru , since spins of $\frac{5}{2}$,¹² $\frac{7}{2}$,^{7, 9, 12, 13, 14} and $\frac{9}{2}$ ¹¹ have been proposed. From the γ -ray anisotropy data of the present work, unique values for the spins of these two ^{101}Ru states can be determined.

III. RESULTS AND DATA ANALYSIS

A. Anisotropy Curves

The temperature dependences of γ -ray anisotropies were measured for the 306.8-keV and 544.8-keV γ lines of ^{101}Ru emitted from a polarized source of Ni($^{101}\text{Rh}^m$). Figure 2 shows the temperature dependence of the anisotropy of the 306.8-keV

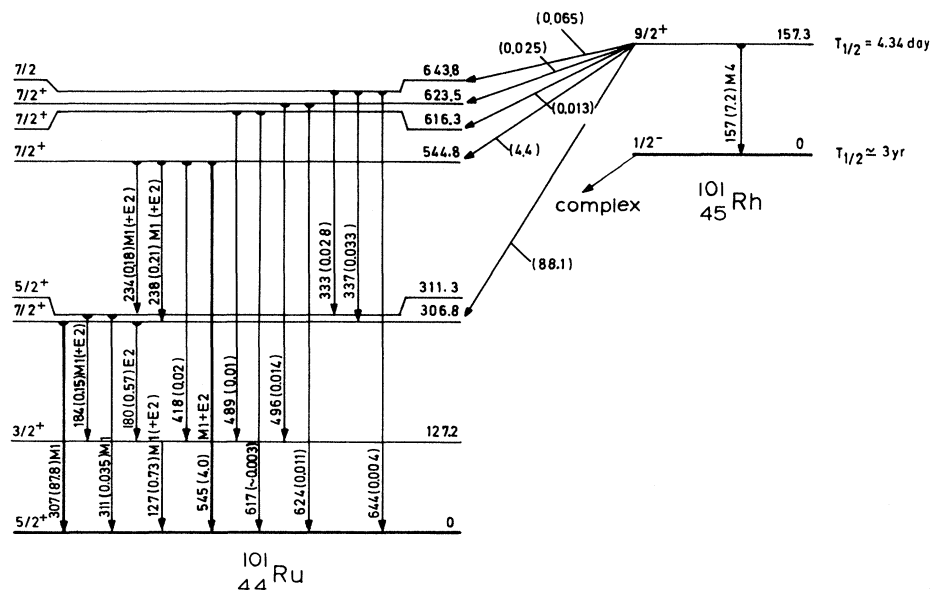


FIG. 1. Decay scheme of $^{101}\text{Rh}^m$ from Ref. 9. Energies are given in keV, and the transition intensities (in % of the total decays) are written in parenthesis.

γ rays emitted parallel ($\theta=0^\circ$) and perpendicular ($\theta=90^\circ$) to the external polarizing field of $H_{\text{ext}}=4$ kOe. The anisotropy of the much weaker 544.8-keV γ line, observed at $\theta=0^\circ$, is shown in Fig. 3 as a function of reciprocal temperature. Here the anisotropy is also positive, but much larger than in the case of the 306.8-keV γ rays. The data for both γ lines were recorded during the warming-up of the sample after a single demagnetization.

In both cases the data were least-squares fitted with the theoretical anisotropy function¹⁵

$$W(\theta) = 1 + \sum_{k=\text{even}} B_k U_k Q_k P_k(\cos\theta), \quad (1)$$

where the P_k are the Legendre polynomials and θ represents the angle between the direction of γ -ray emission and the quantization axis (in the present case identical with the direction of magnetization). The maximum value for k is determined by the spins of the relevant nuclear states and by the multipolarity of the observed γ rays. If parity-violating admixtures in the relevant nuclear states, and hence parity admixtures in the γ -radiation field, can be neglected, only even values of k are permitted. With this assumption only terms with $k=2$ and $k=4$ were taken into account in the present work. The F_k are the angular distribution coefficients for the observed γ transition, the U_k are parameters describing the reorientation of the nucleus due to unobserved preceding decays, and the Q_k are parameters correcting for the finite solid angle of the detector. The orientation of the initial state is described by the orientation param-

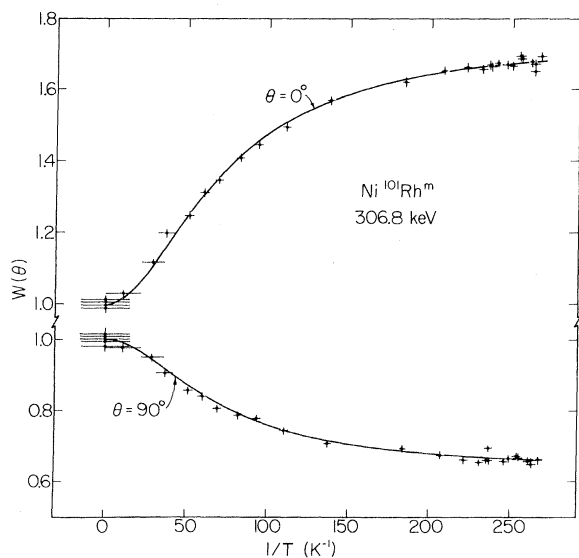


FIG. 2. Temperature dependence of the reduced intensity $W(\theta)$ of the 306.8-keV γ rays from a source of $\text{Ni}^{101}\text{Rh}^m$ of parallel ($\theta=0^\circ$) and perpendicular ($\theta=90^\circ$) to an external polarizing field of 4 kOe.

eters B_k , which are mainly functions of the ratio of the total hyperfine interaction energy $|\mu H_{\text{eff}}|$ to the thermal energy and which are nearly independent of the spin of the isomeric state. Therefore the analysis of the temperature dependence of γ -ray anisotropies yields the absolute value of $|\mu H_{\text{eff}}|$ of the oriented nucleus and provides information on γ -ray multiplicities and level spins.

The solid lines of Fig. 2 are the results of a simultaneous fit of both the 0° and 90° data, using the magnitude of the magnetic hyperfine interaction, $|\mu H_{\text{eff}}|$, and the $E2/M1$ mixing ratio δ ¹⁶ of the 306.8-keV γ line as free adjustable parameters. The spins of $^{101}\text{Rh}^m$ and of the 306.8-keV state of ^{101}Ru were taken as $\frac{9}{2}$ and $\frac{7}{2}$, respectively. The measured anisotropy confirms the spin $I=\frac{7}{2}$ for the 306.8-keV level.

The fitted result for the mixing ratio of the 306.8-keV γ rays,

$$\delta(306.8) = -0.10 \pm 0.05,$$

confirms the predominant $M1$ multipolarity of this γ transition.⁹ For the magnetic hyperfine interaction a value of

$$|\mu H_{\text{eff}}| = (6.20 \pm 0.20) \times 10^{-18} \text{ erg}$$

is obtained.

The large positive anisotropy observed for the 544.8-keV γ line (Fig. 3) completely rules out the values $\frac{5}{2}$ and $\frac{9}{2}$ for the spin of this state. A least-squares fit with $I=\frac{7}{2}$ and with δ as an adjustable parameter yields

$$\delta(544.8) = -0.98 \pm 0.10$$

for the $E2/M1$ mixing ratio of this γ line.

B. NMR-ON Results

Nuclear magnetic resonance of $\text{Ni}^{101}\text{Rh}^m$ was observed at $1/T \approx 200 \text{ K}^{-1}$ by recording the intensity

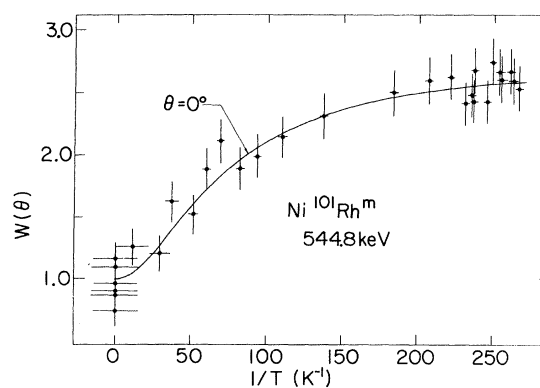


FIG. 3. Temperature dependence of the reduced intensity $W(\theta)$ of the 544.8-keV γ rays from a source of $\text{Ni}^{101}\text{Rh}^m$ parallel ($\theta=0^\circ$) to $H_{\text{ext}}=4$ kOe.

of the 306.8-keV γ line at $\theta=0^\circ$ as a function of the frequency of the applied rf field. In order to make use of a large hyperfine enhancement of the applied rf field, a polarizing field of only 1 kOe was applied to the sample in this case. Figure 4 shows the results of two individual runs with different modulation bandwidths of the rf field. As expected, the experimental linewidth of the resonance curve decreases with decreasing bandwidth. No resonance was detected with an unmodulated rf field, ruling out the possibility of a coil resonance. Whether the resonance curve was measured with increasing or decreasing frequency, the centers of the observed peaks coincided within the present accuracy. This is in agreement with a short nuclear spin-lattice relaxation time, which was found to be less than 30 sec in the temperature range 5 to 10 mK.

From a least-squares fit of the data with Gaussian lines and linear background the resonance fre-

quency was obtained as

$$\gamma_{\text{res}} = 206.2 \pm 0.4 \text{ MHz}.$$

C. Spin and Magnetic Moment of $^{101}\text{Rh}^m$

Table I summarizes the results for the magnetic hyperfine interaction of $\text{Ni}(^{101}\text{Rh}^m)$. The γ -ray anisotropy curves were also least-squares fitted assuming values of $\frac{7}{2}$ and $\frac{11}{2}$ for the spin of $^{101}\text{Rh}^m$, resulting in practically unchanged values for $|\mu H_{\text{eff}}|$. Therefore the results of the NO and NMR-ON measurements can be brought into agreement only if the spin of the isomeric state is equal to $\frac{9}{2}$, in agreement with the earlier spin assignment of Ref. 6. For $I = \frac{9}{2}$ we obtain for the ratio $(\gamma H_{\text{hf}})_{\text{NO}} / (\gamma H_{\text{hf}})_{\text{NMR}}$ a value of 1.02 ± 0.03 , while for $I = \frac{7}{2}$ and $I = \frac{11}{2}$ values of 1.30 ± 0.04 and 0.82 ± 0.03 , respectively, are obtained, ruling out these latter possibilities. In the present case this method of spin determination³⁻⁵ is quite sensitive, due to the small value of the nuclear spin.

For a derivation of a value of the magnetic moment of $^{101}\text{Rh}^m$ from these results a value for the magnetic hyperfine field of rhodium in nickel at very low temperatures is necessary. The hyperfine field of rhodium in nickel has been studied by time-differential perturbed angular correlation with ^{100}Rh up to now only at 77 K and at higher temperatures.¹⁷⁻¹⁹ It was found that the temperature dependence of the reduced hyperfine field $H(T)/H(0)$ follows closely that of the reduced bulk magnetization of nickel metal.¹⁷ At 77 K a hyperfine field of -222 ± 3 kOe has been obtained for $\text{Ni}(\text{Rh})$.^{17, 18} The bulk magnetization of nickel changes by only 0.5% between 77 and 0 K.²⁰ If we assume the same change for the hyperfine field, we obtain an extrapolated value of

$$H_{\text{hf}}(T=0 \text{ K}) = -223 \pm 3 \text{ kOe}$$

which will be used below.

With this value for the hyperfine field of rhodium in nickel a value of

$$\mu(\frac{9}{2}) = (+)(5.51 \pm 0.09) \mu_B$$

can be derived from the present NMR-ON result, taking into account the external polarizing field

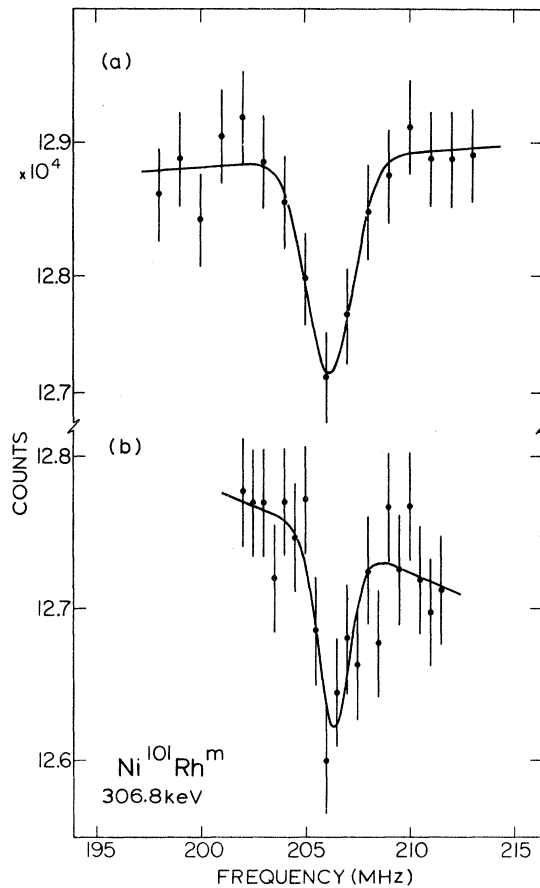


FIG. 4. NMR-ON spectra of the 306.8-keV γ rays of $\text{Ni}(^{101}\text{Rh}^m)$ emitted at $\theta=0^\circ$ relative to the external polarizing field of 1 kOe. The rf frequency was changed in steps of 1 MHz (0.5 MHz) and modulated over a bandwidth of 2 MHz (1 MHz) in spectrum (a) [(b)].

TABLE I. Summary of experimental results for the magnetic hyperfine interaction of $\text{Ni}(^{101}\text{Rh}^m)$.

Method	$ \mu H_{\text{eff}} $ (10^{-18} erg)	Resonance frequency (MHz)
NO	6.2 ± 0.2	...
NMR-ON	(6.147 ± 0.012)	206.2 ± 0.4

of 1 kOe. This magnetic moment corresponds to a nuclear g factor of

$$g\left(\frac{9}{2}\right) = (+)1.22 \pm 0.02.$$

IV. DISCUSSION

According to the shell model the filling of the $1g_{9/2}$ proton shell starts around the proton number $Z=40$, explaining the occurrence of numerous nuclear states with $I^\pi = \frac{9}{2}^+$ in the region around $Z=40$. For quite a large number of these states the nuclear g factors have already been measured. The present results for the spin and magnetic moment of $^{101}\text{Rh}^m$ strongly support an interpretation of this state as a $1g_{9/2}$ proton state, even though the experimental value for the g factor is appreciably smaller than the Schmidt value for the $g_{9/2}$ proton state, $g_{sp} = 1.51$. The deviation of the experimental g factor from the single-particle value has to be interpreted as arising mainly from $M1$ spin polarization²¹ and anomalous proton g_l and g_s factors.²²

It is interesting to compare the present g factor of $^{101}\text{Rh}^m$ with the known g factors of other $1g_{9/2}$ states around $Z=40$. This is done with the help of Fig. 5, where the presently known g factors of $1g_{9/2}$ proton states are plotted versus the proton number. Each of the points in Fig. 5 is labeled with the neutron number of the state involved. For the $\frac{9}{2}^+$ states of $^{71,73,77}\text{As}$,^{23,24} ^{81}Br ,^{25,26} ^{85}Rb ,²⁷ ^{93}Nb ,²³ ^{99}Tc ,²³ and $^{109,111,113,115}\text{In}$ ^{23,28} the measured g factors were used directly, as were the g factors of the 8^+ states of ^{90}Zr ,²² ^{92}Mo ,²² and ^{94}Mo .²⁹

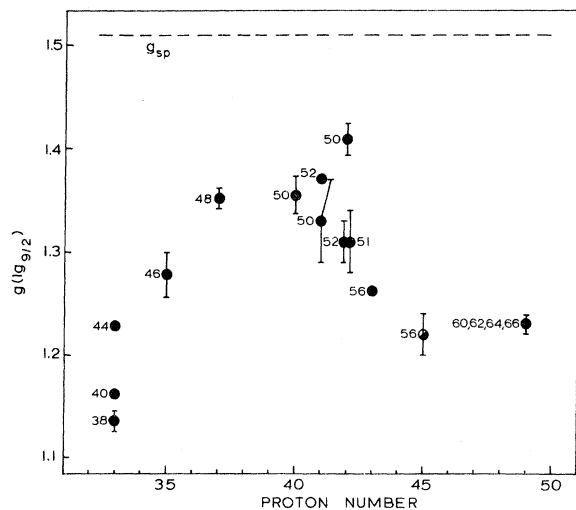


FIG. 5. g factors of $1g_{9/2}$ proton states as a function of the proton number. The respective neutron number is given beside each point. The present result for $^{101}\text{Rh}^m$ (shaded) follows the main trend. For comparison the Schmidt value is also indicated by the dashed line.

A $g_{9/2}$ g factor of 1.33(4) was derived from the $I^\pi = \frac{17}{2}^-$, $g=1.24(4)$, 2368-keV state of ^{91}Nb ,²⁹ based on an interpretation of this state as having a $\{\pi(g_{9/2}^2)8^+; \pi p_{1/2}\}_{17/2^-}$ structure, and assuming $g(p_{1/2}) = -0.275$. Similarly, a $g_{9/2}$ g factor of 1.31(3) was derived from the magnetic moment of the $\frac{21}{2}^+$ state of ^{93}Mo , $\mu\left(\frac{21}{2}^+\right) = 9.21(20)\mu_N$,⁵ assuming a configuration of $\{\pi(g_{9/2}^2)8^+; \nu d_{5/2}\}_{21/1^+}$ and using a value of $-1.30\mu_N$ for the magnetic moment of the $\nu d_{5/2}$ state.³⁰

With increasing proton number, the g factors obviously increase in the region below $Z=40$, while they decrease in the region above (Fig. 5). Qualitatively, such a behavior of g factors is well understood within the concept of $M1$ spin polarization. Considering only protons, the core is closed, even with respect to spin-orbit partners, at the magic proton number $Z=40$, so that $M1$ spin polarization is expected to be smallest there. Going from As ($Z=33$) to Rb ($Z=37$), the effect of $M1$ spin polarization on the g factor will decrease due to the filling up of the p and f shells (blocking). On the other hand, above $Z=40$ the $1g_{9/2}$ shell is being filled, causing the effects of $M1$ spin polarization to increase with the number of protons above $Z=40$ due to $g_{9/2} \rightarrow g_{7/2}$ excitations (enhancement). In principle, the experimental g -factor values should follow a straight line above $Z=40$, where the slope of this line would be a measure for the size of the $M1$ spin polarization in the $1g_{9/2}$ proton shell. In reality (Fig. 5) such a slope is observed, even though there seems to be a spread of g values of the order of 0.1 around the expected straight line, as is clearly shown by the deviations of the g factors of ^{92}Mo , and those of the indium isotopes, from the general trend.

The observed spread in g factors may be caused by a variation of both the neutron and proton configurations. The neutron contributions to the $M1$ spin polarization can be estimated with relatively small uncertainty, since the polarization effects on unlike particles are generally expected to be smaller than on like particles. A mixing of the proton wave function of the type $\alpha\{\pi(p_{1/2})^2; (g_{9/2})^n\} + \beta\{\pi(g_{9/2})^{n+2}\}$ may, however, cause rather large deviations, which can be accounted for only if the wave functions are known, as in the case of ^{93}Nb .²² Using the $M1$ spin-polarization theory of Arima and Horie,²¹ the corrections to the g factor are found to differ by $\Delta g \approx 0.18$ for the two components of the above wave function. This value for Δg is large enough to explain the observed spread in the experimental g factors for $Z > 40$ around a single straight line.

An $M1$ spin-polarization calculation for $^{101}\text{Rh}^m$, using the quoted theory, yields g -factor values of $g=1.29$ for a $\{\pi(p_{1/2})^2; (g_{9/2})^5\}_{9/2^+}$ configuration and

$g=1.10$ for a $\{\pi(g_{9/2})^7\}_{9/2^+}$ configuration, with the experimental value $g=1.22(2)$ lying in between. This may indicate that the wave function of $^{101}\text{Rh}^m$ is a mixture of both configurations. A conclusion of this kind is also supported by the fact that the $\frac{9}{2}^+$ isomeric state of ^{101}Rh lies only 157 keV above the $\frac{1}{2}^-$ ground state.

ACKNOWLEDGMENTS

The authors would like to thank Mrs. Winifred Heppler for her help in chemical separations and Dimitri Voronin for his expertise in mechanical assistance.

†Work performed under the auspices of the U. S. Atomic Energy Commission.

*Present Address: Physik-Department E15, Technische Universität München, D-8046 Garching, West Germany.

‡Present Address: Department of Chemistry, Morehouse College, Georgia 30314.

§Present Address: Hahn-Meitner Institut für Kernforschung, D-1000, Berlin, Germany.

¹D. A. Shirley, *Annu. Rev. Nucl. Sci.* **16**, 89 (1966).

²E. Matthias and R. J. Holliday, *Phys. Rev. Lett.* **17**, 897 (1966).

³F. Bacon, G. Kaindl, H.-E. Mahnke, and D. A. Shirley, *Phys. Rev. Lett.* **28**, 720 (1972).

⁴F. Bacon, G. Kaindl, H.-E. Mahnke, and D. A. Shirley, *Phys. Rev. C* **7**, 1674 (1973).

⁵G. Kaindl, F. Bacon, and D. A. Shirley, *Phys. Rev. C* **8**, 315 (1973).

⁶J. S. Evans, E. Kashy, R. A. Naumann, and R. F. Petry, *Phys. Rev.* **138**, B9 (1965).

⁷N. K. Aras, G. D. O'Kelley, and G. Chilosi, *Phys. Rev.* **146**, 869 (1966).

⁸G. R. Choppin, U. S. Atomic Energy Commission Report No. NAS-NS3008, 1960 (unpublished), Nuclear Science Series (available from Office of Technical Services, U. S. Department of Commerce, Washington, D. C.).

⁹J. Sieniawski, H. Pettersson, and B. Nyman, *Z. Phys.* **245**, 81 (1971).

¹⁰M. E. Phelps and D. G. Sarantites, *Nucl. Phys.* **A159**, 113 (1970).

¹¹J. S. Evans and R. A. Naumann, *Phys. Rev.* **140**, B559 (1965).

¹²O. C. Kistner and A. Schwarzschild, *Phys. Rev.* **154**, 1182 (1967).

¹³B. Siwamogsatham and H. T. Easterday, *Nucl. Phys.*

A162, 42 (1971).

¹⁴C. M. Lederer, J. M. Jaklevic, and J. M. Hollander, *Nucl. Phys.* **A169**, 489 (1971).

¹⁵R. J. Blin-Stoyle and M. A. Grace, *Handb. Phys.* **42**, 555 (1957).

¹⁶K. S. Krane and R. M. Steffen, *Phys. Rev. C* **2**, 724 (1970).

¹⁷R. C. Reno, Ph.D. thesis, Brandeis University, Waltham, Massachusetts (1970).

¹⁸R. C. Reno and C. Hohenemser, in *Hyperfine Interactions in Excited Nuclei*, edited by G. Goldring and R. Kalish (Gordon and Breach, New York, 1971), p. 457.

¹⁹S. Köicki, T. A. Koster, R. Pollak, D. Quitmann, and D. A. Shirley, *Phys. Lett.* **32B**, 351 (1970).

²⁰B. E. Argyle, S. Charap, and E. W. Pugh, *Phys. Rev.* **132**, 2051 (1963).

²¹A. Arima and H. Horie, *Prog. Theor. Phys.* **12**, 623 (1954).

²²S. Nagamiya, T. Katon, T. Nomura, and T. Yamazaki, *J. Phys. Soc. Jap.* **31**, 319 (1970); *Phys. Lett.* **33B**, 574 (1970).

²³V. S. Shirley, in *Hyperfine Interactions in Excited Nuclei* (see Ref. 18), p. 1255.

²⁴D. Quitmann, J. M. Jaklevic, and D. A. Shirley, *Phys. Lett.* **30B**, 329 (1969).

²⁵J. Christiansen, H. Ingwersen, H. G. Johann, W. Klinger, W. Kreische, W. Lampert, G. Schatz, and W. Witthuhn, *Phys. Lett.* **35B**, 501 (1971).

²⁶N. Bräuer, B. Focke, B. Lehmann, K. Nischiyama, and D. Riegel, *Z. Phys.* **244**, 375 (1971).

²⁷W. Bartsch, W. Leitz, H.-E. Mahnke, W. Semmler, R. Sielemann, and Th. Wichert, private communication.

²⁸M. Rice and R. V. Pound, *Phys. Rev.* **106**, 953 (1957).

²⁹F. von Feilitzsch, Diplom-Thesis, Physik-Department, Technische Universität München (1972).

³⁰E. Brun, J. Oeser, and H. H. Staub, *Phys. Rev.* **105**, 1929 (1957).